Phase Behavior, Rheological Property, and Transmutation of Vesicles in Fluorocarbon and Hydrocarbon Surfactant Mixtures

ARTICLE *in* LANGMUIR · MAY 2012

Impact Factor: 4.46 · DOI: 10.1021/la301416e · Source: PubMed

6 AUTHORS, INCLUDING:

Zaiwu Yuan
Qilu University of Technology
14 PUBLICATIONS **165** CITATIONS
SEE PROFILE

Menghua Qin
Taishan University
49 PUBLICATIONS **418** CITATIONS
SEE PROFILE

Hongguang Li
Chinese Academy of Sciences
44 PUBLICATIONS **523** CITATIONS
SEE PROFILE

Langmuir

Article

pubs.acs.org/Langmuir

Phase Behavior, Rheological Property, and Transmutation of Vesicles in Fluorocarbon and Hydrocarbon Surfactant Mixtures

Zaiwu Yuan,[†] Menghua Qin,[†] Xiushan Chen,[†] Changcheng Liu,[‡] Hongguang Li,*[,§] and Jingcheng Hao*[,‡]

[†]School of Chemistry and Pharmaceutical Engineering, Shandong Polytechnic University, Jinan 250353, People's Republic of China

[‡]Key Laboratory of Colloid and Interface Chemistry, Shandong University, Ministry of Education, Jinan 250100, People's Republic of China

[§]State Key Laboratory of Solid Lubrication, Lanzhou Institute of Chemical Physics, Chinese Academy of Sciences, Lanzhou 730000, People's Republic of China

ABSTRACT: We present a detailed study of a salt-free cationic/anionic (catanionic) surfactant system where a strongly alkaline cationic surfactant (tetradecyltrimethylammonium hydroxide, TTAOH) was mixed with a single-chain fluorocarbon acid (nonadecafluorodecanoic acid, NFDA) and a hyperbranched hydrocarbon acid [di-(2-ethylhexyl)phosphoric acid, DEHPA] in water. Typically the concentration of TTAOH is fixed while the total concentration and mixing molar ratio of NFDA and DEHPA is varied. In the absence of DEHPA and at a TTAOH concentration of 80 mmol·L^{-1}, an isotropic L_1 phase, an L_1/L_α two-phase region, and a single L_α phase were observed successively with increasing mixing molar ratio of NFDA to TTAOH (n_{NFDA}/n_{TTAOH}). In the NFDA-rich region ($n_{NFDA}/n_{TTAOH} > 1$), a small amount of excess NFDA can be solubilized into the L_α phase while a large excess of NFDA eventually leads to phase separation. When NFDA is replaced gradually by DEHPA, the mixed system of TTAOH/NFDA/DEHPA/H_2O follows the same phase sequence as that of the TTAOH/NFDA/H_2O system and the phase boundaries remain almost unchanged. However, the viscoelasticity of the samples in the single L_α phase region becomes higher at the same total surfactant concentration as characterized by rheological measurements. Cryo-transmission electron microscopic (cryo-TEM) observations revealed a microstructural evolution from unilamellar vesicles to multilamellar ones and finally to gaint onions. The size of the vesicle and number of lamella can be controlled by adjusting the molar ratio of NFDA to DEHPA. The dynamic properties of the vesicular solutions have also been investigated. It is found that the yield stress and the storage modulus are time-dependent after a static mixing process between the two different types of vesicle solutions, indicating the occurrence of a dynamic fusion between the two types of vesicles. The microenvironmental changes induced by aggregate transitions were probed by ^{19}F NMR as well as ^{31}P NMR measurements. Upon replacement of NFDA by DEHPA, the signal from the ^{19}F atoms adjacent to the hydrophilic headgroup disappears and that from the ^{19}F atoms on the main chain becomes sharper. This could be interpreted as an increase of microfluidity in the mixed vesicle bilayers at higher content of DEHPA, whose alkyl chains are expected to have a lower chain melting point. Our results provide basic knowledge on vesicle formation and their structural evolution in salt-free catanionic surfactant systems containing mixed ion pairs, which may contribute to a deeper understanding of the rules governing the formation and properties of surfactant self-assembly.

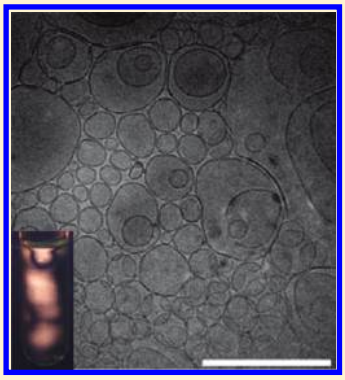

INTRODUCTION

Surfactants, which possess both hydrophobic and hydrophilic parts, have diverse applications in industries and daily life. They can adsorb onto air/water or oil/water interfaces and significantly reduce surface or interface tension. In practical applications, mixed surfactant systems are usually selected because they normally have more advantageous functions compared to systems formed by a single surfactant due to synergistic effects between different components. A typical mixed surfactant system with strong synergistic effects is a cationic/anionic (catanionic) surfactant mixture as pioneered by Kaler et al.[1−9] Upon mixing, a catanionic ion pair is formed, which leads to a strong reduction of the effective area of the hydrophilic headgroup. With the variation of mixing molar ratio, diverse microstructural evolution can be induced. Of special interest is the formation of vesicles, which is a pronounced feature of catanionic surfactant systems. Due to their unique properties, vesicles have practical applications for drug and gene delivery.[10,11] The hydrophobic membrane (called the vesicle wall) can be used to encapsulate oil-soluble organic compounds, while the water pool enclosed by the vesicle walls can be used to encapsulate water-soluble compounds.[12] In addition, vesicles are able to serve as mimics of biological membranes or as micro/nanotemplates for material synthesis.[13−19] However, an obstacle for further investigation and practical application of catanionic surfactant mixtures is precipitate formation, which is more pronounced at high total surfactant concentration and around equimolar

Received: April 6, 2012
Revised: May 29, 2012
Published: May 30, 2012

mixing. One big reason for precipitate formation is the presence of excess inorganic salt formed by small counterions. In recent years, salt-free catanionic surfactant mixtures have received considerable attention. A typical strategy to obtain a salt-free catanionic surfactant system is to use OH^- and H^+ as the counterions of the cationic and anionic surfactant, respectively. Upon mixing, OH^- and H^+ can react to form water. The system thus does not contain excess inorganic salt and the ionic strength of the system is low. By such a method, a variety of salt-free catanionic surfactant systems have been constructed as reported by Hoffmann and co-workers,[20,21] co-workers,[22−25] and our group,[26−30] respectively. Compared to conventional salt-containing catanionic surfactant mixtures, salt-free catanionic surfactant mixtures have a variety of novel properties such as enhanced solubility in water, rich phase behavior with the formation of novel structures, and interesting rheological properties.

To date, the cationic surfactant used in salt-free catanionic surfactant mixtures is typically alkyltrimethylammonium hydroxide and the anionic surfactants are fatty acids with total carbon number ranging from 12 to 18. Recent studies have expanded to novel salt-free catanionic surfactant mixtures containing new and interesting anionic surfactants.[31−35] Although simple salt-free catanionic surfactant mixtures containing only one cationic surfactant and one anionic one have been extensively studied during the past decade, investigation of salt-free catanionic surfactant mixtures containing mixed cationic and/or anionic surfactants with different molecular structures is quite rare. In this work we present a detailed study of a salt-free catanionic surfactant mixture where tetradecyltrimethylammonium hydroxide (TTAOH) is selected as the cationic surfactant and two acids with different molecular structures and properties are selected as anionic surfactants (Scheme 1). NFDA (nonadecafluorodecanoic acid) is a single-chain fluorocarbon carboxylic acid, while DEHPA [di-(2-ethylhexyl)phosphoric acid] is a hyperbranched hydrocarbon phosphoric acid. It is obvious that the length, cross-sectional area, and occupied volume of the hydrophobic part of NFDA and DEHPA are quite different. The fluorocarbon chain is also known to be rigid and immiscible with hydrocarbon chains.[36−39] Thus it is of high interest and importance to investigate the interaction and mutual influences between NFDA and DEHPA in salt-free catanionic surfactant mixtures. The effect is investigated through phase behavior study, rheological measurements, cryo-transmission electron microscopy (cryo-TEM) observations, and NMR measurements. The results are discussed within the theory of critical packing parameter and the spontaneous curvature and fluidity of the molecular bilayers.

Scheme 1. Molecular Structures of TTAOH, NFDA, and DEHPA[a]

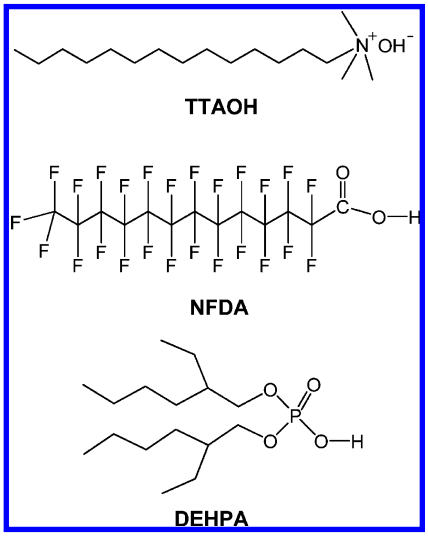

[a]TTAOH, tetradecyltrimethylammonium hydroxide; NFDA, nonadecafluorodecanoic acid; DEHPA, di-(2-ethylhexyl)phosphoric acid. The hydrophilic parts of NFDA and DEHPA are drawn in nondissociated form. Hydrogen atoms in the hydrocarbon chains are omitted for better clarity.

EXPERIMENTAL SECTION

Chemicals and Materials. Tetradecyltrimethylammonium bromide (TTABr) and nonadecafluorodecanoic acid (NFDA) were purchased from Sigma−Aldrich. DEHPA was purchased from Shanghai Chemical Company (China). All chemicals were used as received. TTAOH was prepared from TTABr stock solution by anion exchange (Ion Exchanger III, Merck) following the procedures described previously.[30] D_2O (99.9% deuterated) used for ^{31}P NMR and ^{19}F NMR measurements was obtained from Cambridge Isotope Laboratories, Inc. The water used in the experiments was triply distilled.

Phase Behavior Study. In the phase behavior study, TTAOH stock solutions were prepared first at concentrations of 20, 40, 60, and 80 mmol·L^{-1}. Desired amounts of NFDA or DEHPA or their mixtures were then dissolved in TTAOH stock solutions and the samples were allowed to equilibrate at 25.0 ± 0.5 °C for 10 weeks before further characterization. A phase diagram of TTAOH/NFDA/HDEHP/H_2O was established from observations, both visually and with the help of crossed polarizers, on more than 100 samples.

Rheological Measurements. Rheological measurements were carried out on a Haake RS6000 rheometer with a coaxial cylinder sensor system (Z41 Ti) at 25 °C. The diameters of the rotor and the shear cell are 41.420 and 43.400 mm, respectively. The gap between the inner and outer cylinders is 3 mm. A steady-state shear mode and an oscillation frequency sweep mode were used to measure the rheological properties. An amplitude sweep at a fixed frequency of 1 Hz was performed prior to the following frequency sweep in order to ensure the selected stress was in the linear viscoelastic region. The samples were allowed to equilibrate in the shear cell for 5 min prior to the measurements.

For investigations on the dynamic properties, a static mixing process was adopted. After an adequate equilibration time, the sample formed in TTAOH/NFDA/H_2O system was slowly poured into another sample formed in TTAOH/DEHPA/H_2O system. Then the mixture was gently turned upside-down for several times to get fully mixed. The mixed solution was then divided into three portions with equal volume, which were left for 0, 24, and 72 h, respectively, before rheological measurements.

Cryo-TEM Observations. Samples for cryo-TEM observations were prepared in a controlled environment vitrification system (CEVS) at 25 °C. A microsyringe was used to load 5 μL solution onto a TEM copper grid, which was blotted with two pieces of filter paper, resulting in the formation of thin films suspended on the mesh holes. After about 5 s, the samples were quickly plunged into a reservoir of liquid ethane cooled by liquid nitrogen at −165 °C. The vitrified samples were then

dx.doi.org/10.1021/la301416e | Langmuir 2012, 28, 9355−9364

stored in the liquid nitrogen until they were transferred to a cryogenic sample holder (Gatan 626) and examined with a JEOL JEM-1400 TEM (120 kV) at about −174 °C. The phase contrast was enhanced by underfocus. The images were recorded on a Gatan multiscan charge-coupled device (CCD) and processed with Digital Micrograph. Further information about the cryo-TEM observations can be found elsewhere.[35]

^{31}P NMR and ^{19}F NMR Measurements. ^{31}P NMR and ^{19}F NMR spectra were recorded on a Bruker Avance 400 spectrometer equipped with pulsed-field gradient module (*Z* axis) by use of a 5 mm NMR sample tube. All the sample solutions were dissolved in D_2O and the experiments were operated at 25.0 ± 0.1 °C.

RESULTS AND DISCUSSION

Phase Behavior. First we investigated the phase behavior of the TTAOH/NFDA/H_2O system. Although NFDA is a weak acid, it can react with the strongly alkaline cationic surfactant TTAOH in aqueous solution to form a salt-free catanionic surfactant system. At a TTAOH concentration of 80 mmol·L^{-1}, an isotropic L_1 phase, an L_1/L_α two-phase region, and a single L_α phase were observed successively with increasing mixing molar ratio of NFDA to TTAOH (n_{NFDA}/n_{TTAOH}). In the NFDA-rich region ($n_{NFDA}/n_{TTAOH} > 1$), a small amount of excess NFDA can be solubilized into the L_α phase, while a large excess of NFDA eventually leads to phase separation. When the total concentration of added NFDA is around 100 mmol·L^{-1}, the sample exhibits gel-like behavior and the kinetics of phase separation becomes very slow.

Phase behavior of the TTAOH/DEHPA/H_2O system was included in our previous work.[31,32] In the current work, the phase behavior is studied in further detail at a TTAOH concentration of 80 mmol·L^{-1} for comparison with that of the TTAOH/NFDA/H_2O system. It is found that the phase sequence follows the same order as that observed in the TTAOH/NFDA/H_2O system. Moreover, the phase boundaries also occur in a similar mixing molar ratio of acid to TTAOH. This makes these two systems ideal candidates for investigation of the effects of mixed catanionic ion pairs.

When NFDA is replaced gradually by DEHPA, the mixed system of TTAOH/NFDA/DEHPA/H_2O follows the same phase sequence as that of the TTAOH/NFDA/H_2O system. A typical pseudoternary phase diagram at a TTAOH concentration of 80 mmol·L^{-1} is given in Figure 1. One feature of Figure 1 is that the sum of NFDA and DEHPA (in moles, denoted as $c_{NFDA+DEHPA}$ hereafter) at which phase transition occurs is almost equal to that in the separate system of TTAOH/NFDA/H_2O or TTAOH/DEHPA/H_2O. For example, the single L_α phase can be formed only when $c_{NFDA+DEHPA}$ is in the range of 60−80 mmol·L^{-1} at all mixing molar ratios of NFDA to DEHPA. This can be seen from the relatively straight phase boundary in the phase diagram. It should be mentioned that a similar phenomenon has also been observed at other TTAOH concentrations. This indicates the two catanionic ion pairs, denoted as TTA^+NFD^- and TTA^+DEHP^-, exhibit ideal mixing, though strong synergistic effects exist between the cation and anion within each ion pair. This could be due to the mutual immiscibility between the fluorocarbon chain in NFDA, which is rigid, and the hydrocarbon chains of DEHPA, which are highly flexible.

Cryo-TEM Observations. Although the phase behavior does not change much when NFDA is replaced by DEHPA, the appearance of samples in the L_α phase region exhibits some differences from each other. This is a sign of possible microstructural evolution in the samples induced by the variable composition of the anionic surfactants. To get further details, cryo-TEM observations were carried out on five representative samples in the single L_α phase region, and some typical results are gathered in Figure 2. In the five samples, the concentrations of TTAOH and total anionic surfactants are fixed at 80 and 72 mmol·L^{-1}, respectively, while the mixing molar ratio of DEHPA to NFDA is varied. Closely packed vesicles were observed in all five samples, which is a characteristic property of the L_α phases formed by salt-free catanionic surfactant mixtures around equimolar mixing ratio.[20,21,26−35] Another feature observed from Figure 2 is the dependence of vesicle morphology on the anionic surfactant composition. In the absence of DEHPA (Figure 2a), polydispersed unilamellar vesicles form with diameters ranging from 70 to 250 nm. A few multilamellar vesicles have also been observed. When NFDA was partially replaced by DEHPA, with a molar fraction of DEHPA in the mixed acids [$\rho_{DEHPA} = c_{DEHPA}/(c_{DEHPA} + c_{NFDA})$] of 0.25 (Figure 2b), the dominant vesicles are still unilamellar. However, the vesicles appear to be more polydispersed, which induces a higher packing efficiency. In addition, huge multilamellar vesicles with diameters over 300 nm begin to form. When more NFDA was replaced by DEHPA and the ρ_{DEHPA} reached 0.50 (Figure 2c), the majority of the unilamellar vesicles have transformed to multilamellar ones, which have a higher average diameter. If ρ_{DEHPA} is further increased to 0.75 (Figure 2d), the vesicles begin to deform from the spherical shape, which reveals increased fluidity in the molecular bilayers. Finally, at ρ_{DEHPA} = 1.00, that is, when NFDA is fully replaced by DEHPA (Figure 2e,f) giant multilamellar vesicles (onions) form, with deformed shapes and highly stacked bilayers whose thickness can exceed 100 nm (image e, between the arrows). In some cases, the onion is so big that it can occupy nearly the whole mesh. These results are consistent with literature reports that unilamellar vesicles are usually dominant in catanionic surfactant mixtures containing fluorocarbon surfactant, while giant onions are frequently seen in systems containing flexible alkyl chains.[27,31,40−42]

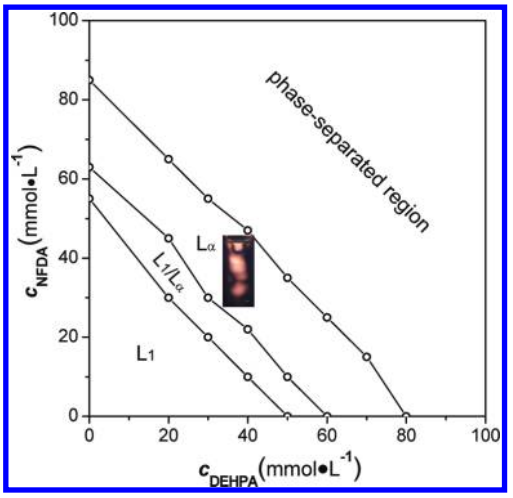

Figure 1. Phase diagram of TTAOH/NFDA/DEHPA/H_2O system at 25.0 ± 0.5 °C at a TTAOH concentration of 80 mmol·L^{-1}. L_1 = isotropic micellar phase; L_α = birefringent vesicular or lamellar phase. (Inset) Picture of a typical sample solution in the single L_α phase region between crossed polarizers, which indicate the birefringence.

dx.doi.org/10.1021/la301416e | *Langmuir* 2012, 28, 9355−9364

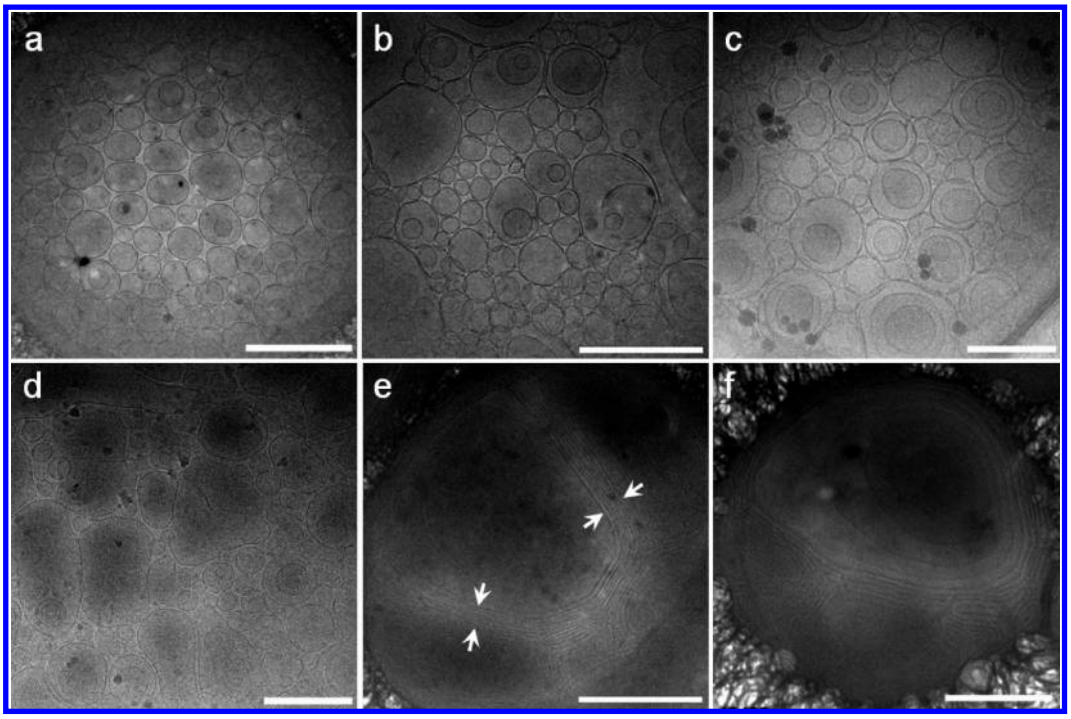

Figure 2. Cryo-TEM images of five typical samples within the L_α phase region. c_{TTAOH} = 80 mmol·L^{-1} and $c_{NFDA+DEHPA}$ = 72 mmol·L^{-1}. ρ_{DEHPA} [= $c_{DEHPA}/(c_{DEHPA} + c_{NFDA})$] = (a) 0, (b) 0.25, (c) 0.50, (d) 0.75, and (e, f) 1.00. The scale bar corresponds to 500 nm.

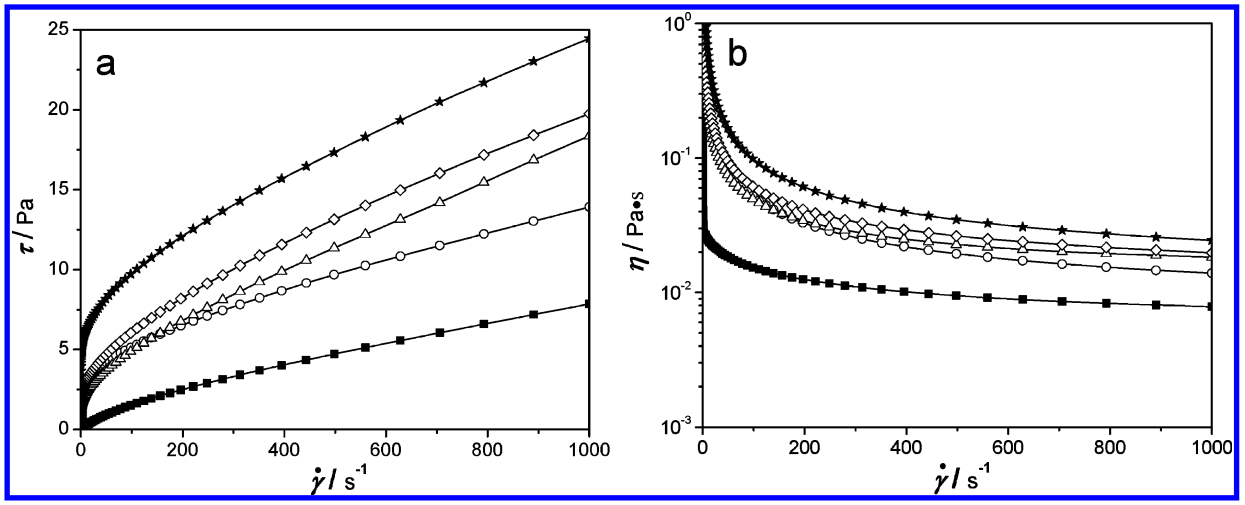

Figure 3. Variation of (a) shear stress and (b) shear viscosity as a function of shear rate for five typical samples within the L_α phase region. c_{TTAOH} = 80 mmol·L^{-1} and $c_{NFDA+DEHPA}$ = 72 mmol·L^{-1}. ρ_{DEHPA} = (■) 0, (○) 0.25, (△) 0.50, (◇) 0.75, and (★) 1.00.

Rheological Properties at Equilibrium State. Rheological measurement is a powerful tool to characterize the characteristics of surfactant solutions, which in many cases are non-Newtonian fluids. Structural evolution occurring in microscopic length scales can have a pronounced influence on the rheological properties of the system. There are already some reports on the rheological properties of surfactant systems containing closely packed vesicles.[20,21,26−35] In these systems the average distance between vesicles is usually much smaller than the average size of the vesicles. Thus, without deformation, the vesicles cannot pass each other and a certain shear stress, regarded as yield stress, is needed to overcome the bending energy of vesicle deformation and initiate a flow.

Figure 3 shows the variation of shear stress (τ) and shear viscosity (η) versus shear rate ($\dot{\gamma}$) of the five representative samples. All five samples show shear-thinning behavior, which is a typical character of vesicular solutions formed by salt-free catanionic surfactant mixtures.[20,21,26−35] In the absence of DEHPA (ρ_{DEHPA} = 0), the sample almost does not exhibit a yield stress. When NFDA is partially replaced by DEHPA and ρ_{DEHPA} equals 0.25, however, an obvious yield stress is observed and the system exhibits the characteristics of Bingham plastic fluids. In addition, the shear stress needed to obtain the same shear rate of the sample also increases, which corresponds to an increase of the shear viscosity. This could be attributed to a more polydispersed size distribution of the vesicles in this stage as proved by cryo-TEM observations (Figure 2b). Since the smaller vesicles can enter the cavities created between the larger vesicles, the packing efficiency of the vesicles is higher, accounting for a higher yield stress and viscosity.

dx.doi.org/10.1021/la301416e | *Langmuir* 2012, 28, 9355−9364

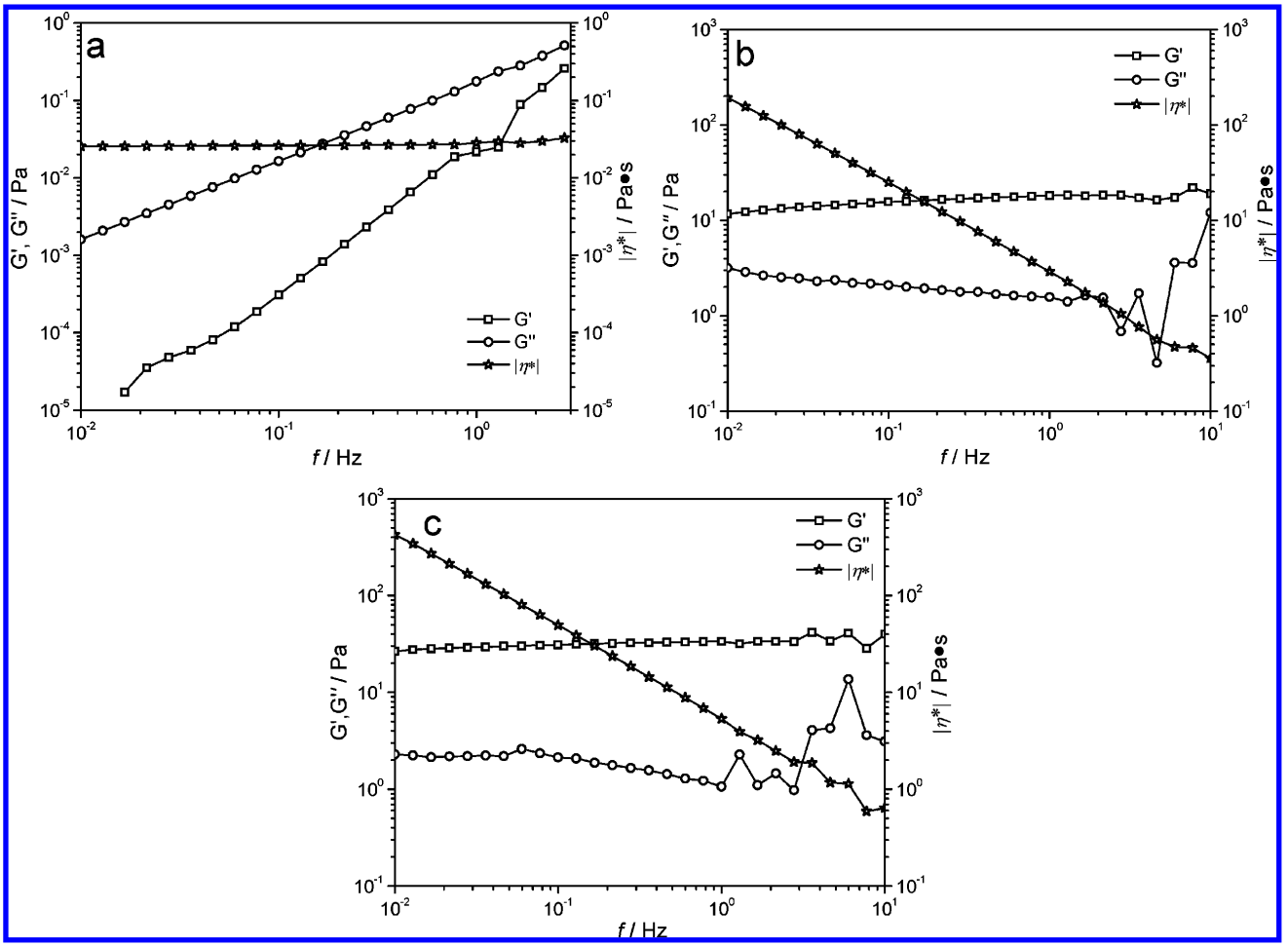

Figure 4. Variation of elastic modulus G', viscous modulus G'', and complex viscosity $|\eta^*|$ as a function of oscillatory frequency for three typical samples in the L_α region. c_{TTAOH} = 80 mmol·L^{-1} and $c_{NFDA+DEHPA}$ = 72 mmol·L^{-1}. ρ_{DEHPA} [= $c_{DEHPA}/(c_{DEHPA} + c_{NFDA})$] = (a) 0, (b) 0.50, and (c) 1.00.

For the three samples with ρ_{DEHPA} = 0.50, 0.75, and 1.00, rheological measurements indicate a continuous increase of yield stress and shear viscosity. From cryo-TEM observations, it is evident that when ρ_{DEHPA} is increased from 0.50 to 1.00, more multilamellar vesicles form and the vesicle size increases continuously. This could be the reason for the increased yield stress and shear viscosity at higher ρ_{DEHPA}, presumably because the giant multilamellar vesicles are more difficult to deform due to the highly stacked bilayers.

Interestingly, when ρ_{DEHPA} is changed from 0.25 to 0.50, an increase in shear viscosity at high shear rates is observed, while at lower shear rates (<150 s^{-1}), an opposite trend is noticed. In addition, the yield stress also slightly decreases with increasing ρ_{DEHPA}. Here we speculate that this phenomenon can be understood by taking into account the special aggregate transition stage within this ρ_{DEHPA} range. From Figure 2 (panels b and c), on one hand the unilamellar vesicles are transforming to multilamellar ones with a larger average size. On the other hand, the polydispersity of the vesicles decreases. Since the former tends to induce an increase in yield stress and shear viscosity while the latter tends to decrease it, the final observation in rheological measurements should be the integrated effect of the two influencing factors.

The effects of ρ_{DEHPA} on rheological properties of the samples also can be probed by the oscillation frequency sweep experiments. Results of three typical samples are shown in Figure 4. In the absence of DEHPA (ρ_{DEHPA} = 0), both the elastic modulus G' and the viscous modulus G'' increase with increasing frequency (Figure 4a). G' is smaller than G'' within the whole investigated frequency range (0.01−10 Hz), demonstrating that the solution is a viscous fluid.[44] When ρ_{DEHPA} is increased to 0.50, a significant increase in both G' and G'' is induced and they become frequency-independent (Figure 4b). Also G' is larger than G'' within the whole frequency range, which indicates the occurrence of a transition from viscous liquid to viscoelastic fluid where the elasticity is dominant.[26,42,43] When ρ_{DEHPA} is further increased to 1.00, the characteristics of the fluid remain similar to what was observed in the sample with ρ_{DEHPA} = 0.50, except for an about 2-fold increase in G'. The fluctuations in G″ at higher frequencies in Figure 4 (panels b and c) should be caused by the instrument, as it becomes difficult to keep a steady shear stress due to the inertia of the rotor.

Kinetic Properties upon Mixing. The rheological properties presented above were obtained from samples prepared by reacting the strongly alkaline cationic surfactant TTAOH and the anionic surfactant mixture. Samples can be also prepared by reacting TTAOH and a single component of anionic surfactant first, and then mixing them together. For example, at a TTAOH concentration of 80 mmol·L^{-1}, the sample with c_{NFDA} = c_{DEHPA} = 36 mmol·L^{-1} (i.e., ρ_{DEHPA} = 0.50) can be equally obtained by mixing the sample with c_{NFDA} = 72 mmol·L^{-1} and c_{DEHPA} = 0

dx.doi.org/10.1021/la301416e | Langmuir 2012, 28, 9355−9364

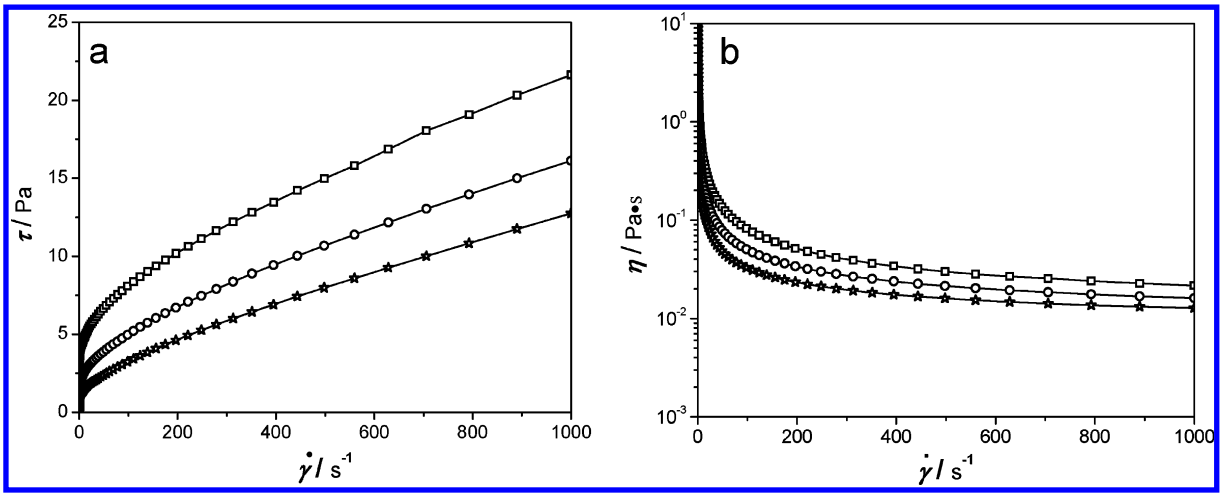

Figure 5. Variation of (a) shear stress and (b) shear viscosity as a function of shear rate for the equivoluminal mixture of two L_α phases formed in TTAOH/NFDA/H_2O and TTAOH/DEHPA/H_2O systems with c_{TTAOH} = 80 mmol·L^{-1} while c_{NFDA} or c_{DEHPA} equals 72 mmol·L^{-1}. Measurements were carried out at postmixing times of (□) 0, (○) 24, and (☆) 72 h.

mmol·L^{-1} and the sample with c_{NFDA} = 72 mmol·L^{-1} and c_{DEHPA} = 0 mmol·L^{-1} in a volume ratio of 1:1. Although the final state after thermodynamic equilibrium should be the same, this latter sample preparation method has the advantage, that is, the kinetic properties of the mixing process of the two vesicular solutions can be conveniently probed by rheological measurements as a function of postmixing time.

Figure 5 shows the variation of the shear stress (τ) and shear viscosity (η) versus shear rate ($\dot{\gamma}$) for the equivoluminal mixture of two above-mentioned samples at different postmixing stages. A continuous decrease in the yield stress and shear viscosity was observed as the postmixing time increased. For example, the yield stress of the sample immediately after mixing is about 5 Pa. After 24 h, the yield stress decreases to about 2.5 Pa. Further aging up to 72 h leads to a smaller yield stress of less than 2 Pa.

The kinetic properties of the mixing process have also been detected by oscillatory stress sweep experiments as shown in Figure 6. At low shear stresses, it is found that the storage modulus G' is higher than the loss modulus G'', and both G' and G'' are almost independent of shear stress. With increasing shear stress, however, G' begins to decrease and, at a critical point, intersects with G''. This intersection point between G' and G'' can be regarded as the maximum shear stress the system can stand, above which microstructural damage will be induced. From Figure 6 one can see that a continuous drop of the maximum shear stress has been induced as the postmixing time increases. In addition, a slight decrease of G' is also observed. This indicates the sample gradually loses its viscoelasticity as a function of time after mixing, which is consistent with the results obtained from steady-state shear mode measurements.

^{19}F and ^{31}P NMR Experiments. It is known that the NMR signals of atoms are sensitive to changes in the physicochemical environment around them. In recent years, NMR measurements on non-hydrogen atoms have become a powerful tool to investigate mixed-surfactant systems.[47] Due to the presence of a fluorocarbon tail in NFDA, ^{19}F NMR was carried out on four typical samples in TTAOH/NFDA/DEHPA/H_2O mixed systems with different compositions, as shown in Figure 7. It can be seen that the signal from α-CF_2 disappears gradually and that from ω-CF_3 undergoes a downfield shift with increasing ρ_{DEHPA}, which is indicative of the changing physicochemical

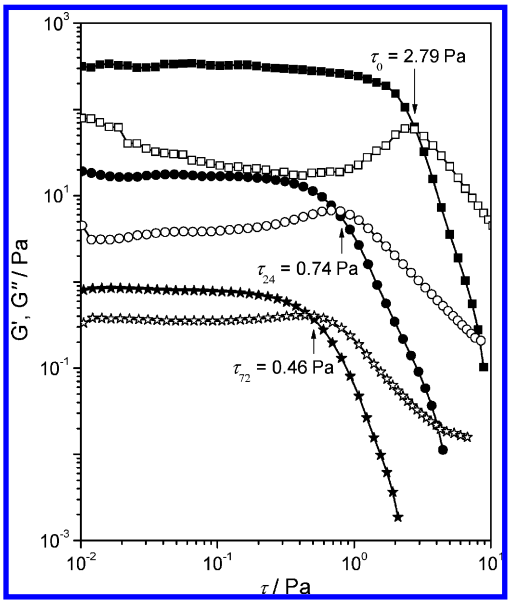

Figure 6. Variation of elastic modulus (G', solid symbols) and viscous modulus (G'', open symbols) as a function of shear stress for the equivoluminal mixture of two L_α phases formed in TTAOH/NFDA/H_2O and TTAOH/DEHPA/H_2O systems with c_{TTAOH} = 80 mmol·L^{-1} while c_{NFDA} or c_{DEHPA} equals to 72 mmol·L^{-1}. Measurements were carried out at postmixing times of (■, □) 0, (●, ○) 24, and (★, ☆) 72 h. The oscillatory frequency is fixed at 1 Hz. The curves obtained at 0 and 72 h were multiplied by factors of 10 and 0.1, respectively, for better clarity.

microenvironment around NFDA molecules. In addition, the signal from β-$(CF_2)_7$ transforms from a broad, multiple peak to a single one at higher ρ_{DEHPA}. It is known that in surfactant aqueous solutions the ^{1}H NMR spectra of the alkyl chains will be broadened once they are embedded in the aggregates.[45−47] The transformation of the signal from β-$(CF_2)_7$ with ρ_{DEHPA} could be caused by a change in microfluidity within the vesicle bilayers. Possessing two hyperbranched alkyl chains, DEHPA has a much lower chain melting temperature compared to that of NFDA. Thus the microfluidity of the mixed vesicle bilayer will increase with increasing ρ_{DEHPA}, accounting for the observed sharper ^{19}F NMR signal at higher ρ_{DEHPA}.

dx.doi.org/10.1021/la301416e | Langmuir 2012, 28, 9355−9364

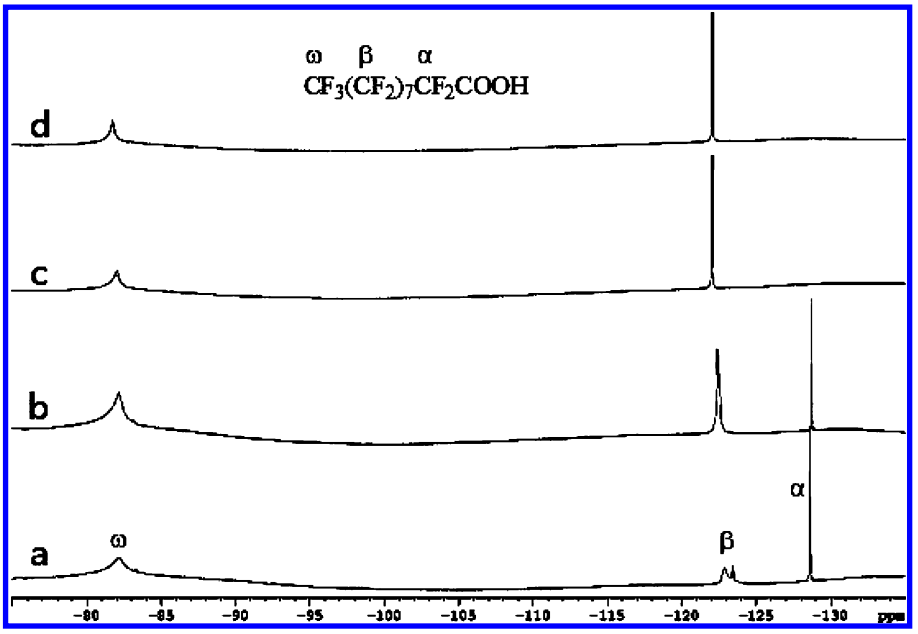

Figure 7. Line profiles of ^{19}F NMR spectra for four NFDA-containing samples. c_{TTAOH} = 80 mmol·L^{-1} and $c_{NFDA+DEHPA}$ = 72 mmol·L^{-1}. ρ_{DEHPA} = (a) 0, (b) 0.25, (c) 0.50, and (d) 0.75.

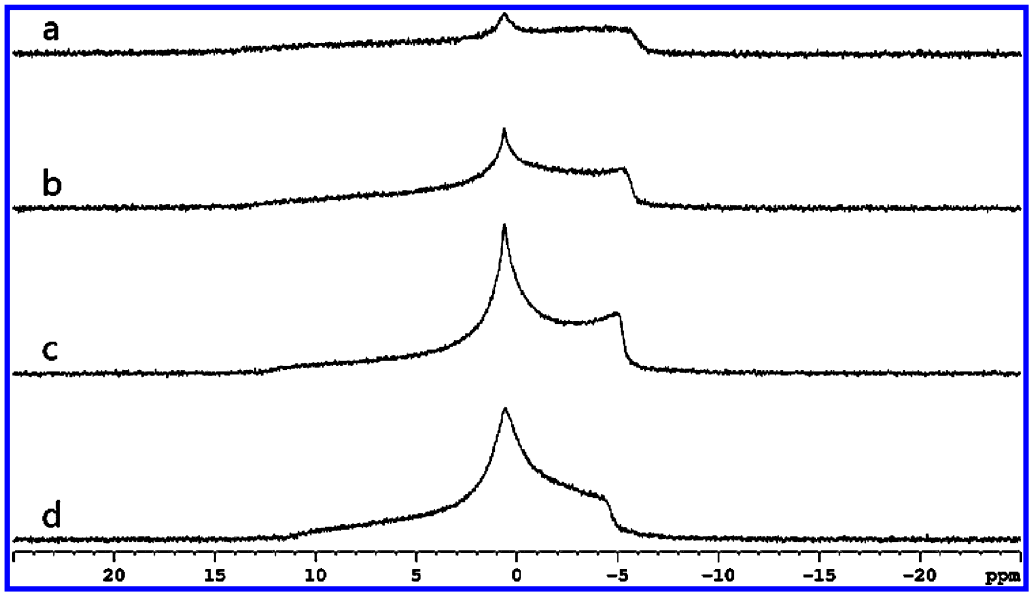

Figure 8. Line profiles of ^{31}P NMR spectra for DEHPA-containing samples. c_{TTAOH} = 80 mmol·L^{-1} and $c_{NFDA+DEHPA}$ = 72 mmol·L^{-1}. ρ_{DEHPA} = (a) 0.25, (b) 0.50, (c) 0.75, and (d) 1.00.

The time-averaged environments for DEHPA in vesicles can be detected through the ^{31}P NMR spectra. Results obtained from four typical samples are given in Figure 8, from which one can see the ^{31}P chemical shift remains almost invariable in the four samples due to the similar anisotropy for the vesicular self-assemblies.[46] However, the intensity of the ^{31}P signal becomes stronger at higher ρ_{DEHPA} due to an increasing amount of phosphorus atoms available for NMR detection. The width of the ^{31}P NMR peaks is known to be dependent on the exchange rate of the phosphorus-containing surfactants between the surfactant aggregates on the NMR time scale.[47] From Figure 8 one can also see that all the ^{31}P NMR spectra for the four samples are broad. This could be due to the high viscoelasticity of the vesicle solutions, which induces a low exchange rate of the DEHPA molecules between vesicles.

Further Discussion. From the above observations, an interesting microstructure transition in the salt free catanionic surfactant system can be obtained when the fluorocarbons are replaced by hydrocarbons. It was found that unilamellar vesicles will be replaced by multilamellar ones if fluorocarbons are replaced with hydrocarbons. There are two possible mechanisms for vesicle formation in TTAOH/NFDA/DEHPA/H_2O mixed systems. Containing one strongly alkaline cationic surfactant and two anionic surfactants, which are weak acids, catanionic ion pairs of TTA^+NFD^- and TTA^+DEHP^- can form due to the electrostatic interactions (Scheme 2). On the basis of cryo-TEM observations, it can be speculated that the two catanionic ion pairs can mix together and form vesicles instead of forming vesicles individually, because the vesicles observed in TTAOH/NFDA/DEHPA/H_2O mixed system cannot be

dx.doi.org/10.1021/la301416e | *Langmuir* 2012, 28, 9355−9364

Scheme 2. Illustration of Formation of Catanionic Ion Pairs[a]

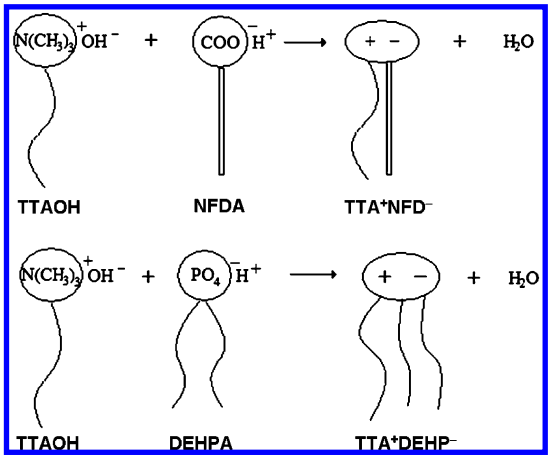

[a]The acid−base reactions between TTAOH and NFDA or DEHPA produced two different types of catanionic ion pairs bearing double and triple chains, respectively. The hydrophilic parts of NFDA and DEHPA were drawn in dissociated form to facilitate the acid−base reaction. The hydrocarbon chains are presented as flexible lines while the fluorocarbon chains are illustrated as rigid rods. For better clarity, the side chains on the hydrocarbon tails of DEHPA have been omitted.

regarded as a physical mixture of the two types of vesicles formed in the TTAOH/NFDA/H_2O system and the TTAOH/DEHPA/H_2O system.

According to the curvature free-energy equation,[2,40,48]

$$f = 2K\left(\frac{1}{R} - \frac{1}{R_0}\right)^2$$

where f is the curvature energy per unit area of vesicle bilayer, K is an effective bending constant, R is the vesicle radius, and R_0 is the radius of the vesicle with minimum energy. The microstructures of vesicles are mainly determined by (i) spontaneous curvature $(1/R_0)$ of the surfactant bilayers, which chooses the optimum radius (R_0) of vesicles and decides the vesicle sizes basically, and (ii) effective bending constant (K), which represents the curvature elasticity or rigidity of the vesicle bilayers and governs the polydispersity of vesicles. In the current case, the single-tailed NFDA is expected to have a smaller critical packing parameter p $(= v/a_0l_c$, where v and l_c are the volume and length of the hydrophobic alkyl chain and a_0 is the effective cross-sectional area of the hydrophilic headgroup.[49]) than that of the double-tailed DEHPA. On the other hand, the fluorocarbon chain in NFDA is much stiffer than the branched hydrocarbon chains in DEHPA. Therefore, vesicles containing more NFDA have a smaller R_0 and a larger K, which is responsible for the formation of the smaller-sized unilamellar vesicles when mixed with TTAOH in aqueous solutions. On the contrary, DEHPA has a larger p, resulting in a larger spontaneous radius R_0, and at the same time, the hydrocarbon chains of DEHPA are relatively softer than that of NFDA. The above effects lead to the formation of larger-sized multilamellar vesicles when DEHPA is mixed with TTAOH in aqueous solutions. Indeed, catanionic surfactant mixtures with flexible alkyl chains have a propensity to form onions.[27] The replacement of NFDA by DEHPA can enhance the spontaneous radius and at the same time lower the bending constant of vesicle bilayers, leading to the formation of larger multilamellar vesicles with increasing content of DEHPA. Besides the explanation by curvature energy change in this process, many other factors, especially the interaction between the hydrophobic chains, should be considered in the current surfactant system. We also expect that the mutual phobic nature between hydrocarbons and fluorocarbons would be more crucial in explaining this transition from unilamellar vesicles to multilamellar ones if fluorocarbons are replaced with hydrocarbons. Where fluorocarbon is involved, not only can the packing parameter be cited but also the interaction between hydrocarbons and fluorocarbons should be considered.

CONCLUSION

We have investigated the phase behavior and microstructural evolution in a salt-free catanionic surfactant system containing one strongly alkaline cationic surfactant and two weakly acidic anionic surfactants with distinct molecular morphologies and properties. It is found that the morphologies of vesicles formed in this system can be controlled by adjusting the mixing molar ratio of the anionic surfactants. At the fluorocarbon acid NFDA-rich side, polydispersed unilamellar vesicles are dominant. Upon replacement of NFDA with the hydrocarbon acid DEHPA, aggregate transition from unilamellar vesicles to multilamellar ones and then to giant onions with deformed shapes has been detected by cryo-TEM observations. This microstructural evolution has resulted in a drastic change in the rheological properties of the system and can be also probed by ^{19}F and ^{31}P NMR measurements. The control mechanism is based on regulation of the spontaneous curvature radius, the curvature elasticity of vesicles, and even the interaction between hydrocarbons and fluorocarbons of surfactant mixtures. Our results can primarily provide a deeper understanding of the transition between bilayer structures in aqueous solutions governed by surfactant molecular structures and secondarily contribute to the realization of practical applications of salt-free catanionic surfactant mixtures, which have attracted increasing interest in recent years.

AUTHOR INFORMATION

Corresponding Author

*E-mail hgli@licp.cas.cn or jhao@sdu.edu.cn; tel +86-531-88366074.

Notes

The authors declare no competing financial interest.

ACKNOWLEDGMENTS

This work was financially supported by the NSFC (Grant 21033005) and the National Basic Research Program of China (973 Program, 2009CB930103), and NFS of Shandong Province (2009ZRB01876).

REFERENCES

(1) Kaler, E. W.; Herrington, K. L.; Murthy, A. K.; Zasadzinski, J. A. N. Spontaneous Vesicle Formation in Aqueous Mixtures of Single-Tailed Surfactants. *Science* **1989**, *245*, 1371−1374.

(2) Safran, S. A.; Pincus, P.; Andelman, D. Theory of Spontaneous Vesicle Formation in Surfactant Mixtures. *Science* **1990**, *248*, 354−356.

(3) Kaler, E. W.; Herrington, K. L.; Murthy, A. K. Phase Behavior and Structures of Mixtures of Anionic and Cationic Surfactants. *J. Phys. Chem.* **1992**, *96*, 6698−6707.

(4) Herrington, K. L.; Kaler, E. W.; Miller, D. D.; Zasadzinski, J. A.; Chiruvolu, S. Phase Behavior of Aqueous Mixtures of Dodecyltrimethylammonium (DTAB) and Sodium Dodecyl Sulfate (SDS). *J. Phys. Chem.* **1993**, *97*, 13792−13802.

(5) Yatcilla, M. T.; Herrington, K. L.; Brasher, L. L.; Kaler, E. W.; Chiruvolu, S.; Zasadzinski, J. A. Phase Beahvior of Aqueous Mixtures of Cetyltrimethylammonium (CTAB) and Sodium Octyl Sulfate (SOS). *J. Phys. Chem.* **1996**, *100*, 5874−5879.
(6) Iampietro, D. J.; Kaler, E. W. Phase Behavior and Microstructure of Aqueous Mixtures of Cetyltrimethylammonium Bromide and Sodium Perfluorohexanoate. *Langmuir* **1999**, *15*, 8590−8601.
(7) Koehler, R. D.; Raghavan, S. R.; Kaler, E. W. Microstructure and Dynamics of Wormlike Micellar Solutions Formed by Mixing Cationic and Anionic Surfactants. *J. Phys. Chem. B* **2000**, *104*, 11035−11044.
(8) Raghavan, S. R.; Fritz, G.; Kaler, E. W. Wormlike Micelles Formed by Synergistic Self-Assembly in Mixtures of Anionic and Cationic Surfactants. *Langmuir* **2002**, *18*, 3797−3803.
(9) Schubert, B. A.; Kaler, E. W.; Wagner, N. J. The Miscrostructure and Rheology of Mixed Cationic/Anionic Wormlike Micelles. *Langmuir* **2003**, *19*, 4079−4089.
(10) Lasic, D. D. Novel Applications of Liposomes. *Trends Biotechnol.* **1998**, *16*, 307−321.
(11) Torchilin, V. P. Recent Advances with Liposomes as Pharmaceutical Carriers. *Nat. Rev. Drug. Discovery* **2005**, *4*, 145−160.
(12) Nii, T.; Ishii, F. Encapsulation Efficiency of Water-Soluble and Insoluble Drugs in Liposomes Prepared by the Microencapsulation Vesicle Method. *Int. J. Pharm.* **2005**, *298*, 198−205.
(13) Lipowsky, R.; Sackmann, E. *Structure and Dynamics of Membranes; From Cells to Vesicles*; Handbook of Biological Physics, Vol. *1*; Elsevier: Amsterdam, 1995.
(14) Marques, E. F. Size and Stability of Catanionic Vesicles: Effects of Formation Path, Sonication, and Aging. *Langmuir* **2000**, *16*, 4798−4807.
(15) Rosoff, M., Ed. *Vesicles*; Surfactant Science Series 62, Marcel Dekker: New York, 1996.
(16) Hentze, H. P.; Raghavan, S. R.; McKelvey, C. A.; Kaler, E. W. Silica Hollow Spheres by Templating of Catanionic Vesicles. *Langmuir* **2003**, *19*, 1069−1074.
(17) Hao, J.; Wang, J.; Liu, W.; Abdel-Rahem, R.; Hoffmann, H. Zn^{2+}-Induced Vesicle Formation. *J. Phys. Chem. B* **2004**, *108*, 1168−1172.
(18) Hubert, D. H. W.; Jung, M.; German, A. L. Vesicle Templating. *Adv. Mater.* **2000**, *12*, 1291−1294.
(19) Yeh, Y. Q.; Chen, B. C.; Lin, H. P.; Tang, C. Y. Synthesis of Hollow Silica Spheres with Mesostructured Shell Using Cationic−Anionic−Neutral Block Copolymer Ternary Surfactants. *Langmuir* **2006**, *22*, 6−9.
(20) Horbaschek, K.; Hoffmann, H.; Thunig, C. Formation and Properties of Lamellar Phases in Systems of Cationic Surfactants and Hydroxy-Naphthoate. *J. Colloid Interface Sci.* **1998**, *206*, 439−456.
(21) Horbaschek, K.; Hoffmann, H.; Hao, J. Classic L_α Phases as Opposed to Vesicle Phases in Cationic−Anionic Surfactant Mixtures. *J. Phys. Chem. B* **2000**, *104*, 2781−2784.
(22) Zemb, Th.; Dubois, M.; Demé, B.; Gulik-Krzywicki, Th. Self-Assembly of Flat Nanodiscs in Salt-Free Catanionic Surfactant Solutions. *Science* **1999**, *283*, 816−819.
(23) Dubois, M.; Demé, B.; Gulik-Krzywicki, Th.; Dedieu, J. C.; Vautrin, C.; Désert, S.; Perez, E.; Zemb, Th. Self-assembly of Regular Hollow Icosahedra in Salt-Free Catanionic Solutions. *Nature* **2001**, *411*, 672−675.
(24) Meister, A.; Dubois, M.; Belloni, L.; Zemb, Th. Equation of State of Self-Assembled Disklike and Icosahedral Crystallites in the Dilute Range. *Langmuir* **2003**, *19*, 7259−7263.
(25) Dubois, M.; Lizunov, V.; Meister, A.; Gulik-Krzywicki, Th.; Verbavatz, J. M.; Perez, E.; Zimmerberg, J.; Zemb, Th. Shape Control through Molecular Segregation in Giant Surfactant Aggregates. *Proc. Natl. Acad. Sci. U.S.A.* **2004**, *101*, 15082−15087.
(26) Hao, J.; Liu, W.; Xu, G.; Zheng, L. Vesicles from Salt-Free Cationic and Anionic Surfactant Solutions. *Langmuir* **2003**, *19*, 10635−10640.
(27) Song, A.; Dong, S.; Jia, X.; Hao, J.; Liu, W.; Liu, T. An Onion Phase in Salt-Free Zero-Charged Catanionic Surfactant Solutions. *Angew. Chem., Int. Ed.* **2005**, *44*, 4018−4021.
(28) Yuan, Z.; Hao, J.; Hoffmann, H. A Promising System of Mixed Single- and Double-Short-Tailed PEO Ether Phosphate Esters: Phase Behavior and Vesicle Formation. *J. Colloid Interface Sci.* **2006**, *302*, 673−681.
(29) Shen, Y.; Hao, J.; Hoffmann, H. Reversible Phase Transition between Salt-Free Catanionic Vesicles and High-Salinity Catanionic Vesicles. *Soft. Matter.* **2007**, *3*, 1407−1412.
(30) Li, H.; Hao, J. Phase Behavior and Rheological Properties of a Salt-Free Catanionic Surfactant TTAOH/LA/H_2O System. *J. Phys. Chem. B* **2008**, *112*, 10497−10508.
(31) Yuan, Z.; Yin, Z.; Sun, S.; Hao, J. Densely Stacked Multilamellar and Oligovesicular Vesicles, Bilayer Cylinders, and Tubes Joining with Vesicles of a Salt-Free Catanionic Extractant and Surfactant System. *J. Phys. Chem. B* **2008**, *112*, 1414−1419.
(32) Yuan, Z.; Dong, S.; Liu, W.; Hao, J. Transition from Vesicle Phase to Lamellar Phase in Salt-Free Catanionic Surfactant Solution. *Langmuir* **2009**, *25*, 8974−8981.
(33) Zhang, J.; Song, A.; Li, Z.; Xu, G.; Hao, J. Phase Behaviors and Self-Assembly Properties of Two Catanionic Surfactant Systems: $C_8F_{17}COOH/TTAOH/H_2O$ and $C_8H_{17}COOH/TTAOH/H_2O$. *J. Phys. Chem. B* **2010**, *114*, 13128−13135.
(34) Liu, C.; Hao, J. Influence of Cholic Acid on Phase Transition, Rheological Behavior, and Microstructures of Salt-Free Catanionic Surfactant Mixtures. *J. Phys. Chem. B* **2010**, *114*, 4477−4484.
(35) Liu, C.; Hao, J. Shear-Induced Structural Transition and Recovery in the Salt-Free Catanionic Surfactant Systems Containing Deoxycholic Acid. *J. Phys. Chem. B* **2011**, *115*, 980−989.
(36) Almgren, M.; Garamus, V. M. Small Angle Neutron Scattering Study of Demixing in Micellar Solutions Containing CTAC and a Partially Fluorinated Cationic Surfactant. *J. Phys. Chem. B* **2005**, *109*, 11348−11353.
(37) Nordstierna, L.; Furó, I.; Stilbs, P. Mixed Micelles of Fluorinated and Hydrogenated Surfactants. *J. Am. Chem. Soc.* **2006**, *128*, 6704−6712.
(38) Blanco, E.; Messina, P.; Ruso, J. M.; Prieto, G.; Sarmiento, F. Regarding the Effect that Different Hydrocarbon/Fluorocarbon Surfactant Mixtures Have on Their Complexation with HSA. *J. Phys. Chem. B* **2006**, *110*, 11369−11376.
(39) Peyre, V.; Patil, S.; Durand, G.; Pucci, B. Mixtures of Hydrogenated and Fluorinated Lactobionamide Surfactants with Cationic Surfactants: Study of Hydrogenated and Fluorinated Chains Miscibility through Potentiometric Techniques. *Langmuir* **2007**, *23*, 11465−11474.
(40) Jung, H. T.; Coldren, B.; Zasadzinski, J. A.; Iampietro, D. J.; Kaler, E. W. The Origins of Stability of Spontaneous Vesicles. *Proc. Natl. Acad. Sci. U.S.A.* **2001**, *98*, 1353−1362.
(41) Jung, H. T.; Lee, S. Y.; Kaler, E. W.; Coldren, B.; Zasadzinski, J. A. Gaussian Curvature and the Equilibrium among Bilayer Cylinders, Spheres, and Discs. *Proc. Natl. Acad. Sci. U.S.A.* **2002**, *99*, 15318−15322.
(42) Li, X.; Dong, S.; Jia, X.; Song, A.; Hao, J. Vesicles of a New Salt-Free Catanionic Fluoro/Hydrocarbon Surfactant System. *Chem.—Eur. J.* **2007**, *13*, 9495−9502.
(43) Sollich, P.; Lequeux, F.; Hébraud, P.; Cates, M. E. Rheology of Soft Glassy Materials. *Phys. Rev. Lett.* **1997**, *78*, 2020−2023.
(44) Steffe, J. F. *Rheological Methods in Food Process Engineering*; Freeman Press: East Lansing, MI, 1996.
(45) Menger, F. M.; Littau, C. A. Gemini Surfactants: A New Class of Self Assembling Molecules. *J. Am. Chem. Soc.* **1993**, *115*, 10083−10090.
(46) Gustafsson, J.; Orädd, G.; Lindblom, G.; Olsson, U.; Almgren, M. A Defective Swelling Lamellar Phase. *Langmuir* **1997**, *13*, 852−860.
(47) Dong, S.; Xu, G.; Hoffmann, H. Aggregation Behavior of Fluorocarbon and Hydrocarbon Cationic Surfactant Mixtures: A Study of ^1H NMR and ^{19}F NMR. *J. Phys. Chem. B* **2008**, *112*, 9371−9378.
(48) Helfrich, W. Elastic Properties of Lipid Bilayers: Theory and Possible Experiments. *Z. Naturforsch.* **1973**, *28*, 693−703.

(49) Israelachvili, J. N.; Mitchell, D. J.; Ninham, B. W. Theory of Self-Assembly of Hydrocarbon Amphiphiles into Micelles and Bilayers. *J. Chem. Soc., Faraday Trans. 2* **1976**, *72*, 1525−1568.